# Dependence of Electrical Properties of InAlN/GaN and InAlN/AlGaN/GaN Heterostructures FETs on the AlN Interlayer Thickness

**Masanobu HIROKI**[†a)], **Narihiko MAEDA**[†], ***Nonmembers, and* Naoteru SHIGEKAWA**[†], *Member*

**SUMMARY**   We investigated the influence of the thickness of the AlN interlayer for InAlN/GaN and InAlN/AlGaN/GaN heterostructures. The AlN thickness strongly affects the surface morphology and electron mobility of the InAlN/GaN structures. The rms roughness of the surface increases from 0.35 to 1.2 nm with increasing AlN thickness from 0 to 1.5 nm. Large pits are generated when the AlN is thicker than 1 nm. The highest electron mobility of 1470 cm$^2$/V·s is obtained for a 0.75-nm-thick AlN interlayer. The mobility, however, becomes lower with increasing deviation from 0.75 nm. It is only 200 cm$^2$/V·s for the 0-nm thick AlN. Inserting AlGaN between AlN and InAlN suppresses the influence of the AlN interlayer thickness. A smooth surface with rms roughness of 0.35 nm is obtained for all samples with 0–1.5-nm-thick AlN. The electron mobility ranges from 1000 to 1690 cm$^2$/V·s. The variation is smaller than that for InAlN/GaN. We fabricated field effect transistors (FETs) with gate length of 2 $\mu$m. The electron mobility in the access region affects the transconductance ($g_m$) of FETs. As a results, the influence of the AlN thickness for InAlN/GaN FETs is larger than that for InAlN/AlGaN/GaN FETs, which reduces gate leakage current. The transconductance varies from 93 to 235 mS/mm for InAlN/GaN FETs. In contrast, it varies from 180 to 230 mS/mm for InAlN/AlGaN/GaN FETs. These results indicate that the InAlN/AlGaN/GaN heterostructures could lead to the development of GaN-based FETs.

***key words:*** *GaN-based FETs, HEMTs, InAlN, AlInN, AlGaN*

## 1. Introduction

GaN-based field effect transistors (FETs) are attractive for high-frequency and high-power devices because of their high electron saturation velocity and high critical electric field. AlGaN/GaN heterostructures are conventionally used for the FETs. The polarization effect is an important characteristic of the III-nitride semiconductor heterostructures. Spontaneous and piezoelectric polarization induces an internal electric field due to the polarity of the wurtzite structure and large electronegativity of nitrogen atoms [1], [2]. The large charge induced by the difference in the polarization between the barrier layer and the buffer layer generates a large density of two-dimensional electron gas ($N_S$). Therefore, $N_S$, which affects the threshold voltage and the sheet resistance, varies with the composition and thickness of the barrier layer. InAlN is attractive as a barrier layer for controlling the polarization charge. InAlN with In content of 0.17–0.18, lattice-matched to GaN, has a large spontaneous

polarization charge of 0.072 C/m$^2$. This results in the generation of large $N_S$ of about $2.5 \times 10^{13}$ cm$^{-2}$ at the heterointerface without lattice strain [3], [4]. Therefore, we can fabricate FETs with low channel resistance and high reliability. On the other hand, the polarization charge of compressively strained InAlN with In content of about 0.32 should be equal to that of GaN [4]. In this case, two-dimensional electron gas can be eliminated at the heterointerface. Therefore, compressively strained InAlN/GaN heterostructures can be used for normally-off operation devices.

However, there are some problems with InAlN/GaN heterostructures. One is that InAlN growth is difficult because of low growth temperature of around 800°C. A high growth temperature of over 1000°C is needed in order to grow high-quality Al-rich nitride semiconductor due to the low migration length of Al atoms and strong atomic bonds of AlN. However, such a high temperature inhibits incorporation of In into the solid phase [5]. Thus, InAlN must be grown at low temperature of around 800°C, which degrades the crystal quality of InAlN and makes it difficult to control the In content. We have optimized the MOVPE growth condition and can control the In content in the region from 0.13 to 0.33. Another problem is the low electron mobility for InAlN/GaN heterostructures. It has been predicted that the alloy-disorder scattering rate in InAlN is extremely large [6]. Therefore, the electron mobility is suppressed at around 200 cm$^2$/V·s for InAlN/GaN heterostructures. To boost the mobility, an AlN interlayer has been widely used [7]–[9]. The AlN interlayer of binary alloy can suppress alloy disorder scattering, and it increases the effective conduction-band offset because of the large polarization charge [10], [11]. The electron mobility is as high as 1300 cm$^2$/V·s for InAlN/AlN/GaN heterostructures [9]. Howerver, the surface tends to be rough and have large pits due to the roughness of the AlN interlayer. To solve this problem, we have fabricated InAlN/AlGaN/AlN/GaN heterostructures [12], [13]. The inserted AlGaN layer smooths out the rough AlN surface, resulting in a flat InAlN surface and an abrupt heterointerface. We were therefore able to achieve a flat surface and high electron mobility for InAlN/AlGaN/AlN/GaN heterostructures.

The thickness of the AlN interlayer is especially important for improving the properties of the heterostructures with an InAlN barrier. It has been reported that AlN interlayer thickness sensitively affects the surface flatness and

mobility [9]. In addition, the insertion of an AlN interlayer has been shown to decrease the reliability for AlGaN/GaN heterostructures FETs [14]. The effective conduction-band offset is extremely sensitive to AlN interlayer thickness because of the large polarization charge; therefore, the atomic fluctuation of AlN interlayer results in the local breakdown of the gate finger. This finding indicate that no AlN interlayer is preferable from the view-point of reliability. In this study, we investigated the effect of AlN thickness for lattice-matched (LM) InAlN/GaN and InAlN/AlGaN/GaN heterostructures. We found that the insertion of AlGaN suppresses the influence of the AlN thickness.

## 2. Experimental

The heterostructures were fabricated by low-pressure vertical metal organic vapor phase epitaxy (MOVPE) on sapphire substrate. Trymethylgalium, trymethyl aluminum, trymethylindium, and ammonia were the precursors of Ga, Al, In, and N, respectively. First, we grew a 2-$\mu$m-thick GaN buffer layer at about 1000°C and 300 Torr. Next, we reduced the pressure to 200 Torr and deposited an AlN layer to a thickness between 0 to 1.5 nm and a 5-nm-thick $Al_{0.38}Ga_{0.62}N$ layer. Then, we cooled the wafers down to 730–800°C, reduced the pressure to 110 Torr, and switched the carrier gas from $H_2$ to $N_2$ for the growth of the LM-InAlN layer, which has In content of 0.17–0.18 and a thickness of 8–12 nm. For comparison, we also fabricated InAlN/AlN/GaN heterostructures with the thickness of 15–20 nm using the same growth procedure. From the band-profile calculation, we found that $N_S$ increases with increasing Al content, indicating that high Al content in AlGaN is preferable for obtaining large $N_S$. In this study, we therefore used 0.38, which is the highest value obtainable in our growth system [12].

We observed the surface morphology by atomic force microscopy (AFM) and estimated $N_S$ and the electron mobility from Hall effect measurements in the Van der Pauw configuration. We characterized the composition of InAlN by x-ray diffraction (XRD), secondary ion mass spectroscopy (SIMS), and Rutherford backscattering spectroscopy (RBS). We fabricated HFETs using photolithography and lift-off techniques. We used ion-coupled-plasma etching with $Cl_2$ gas to isolate devices and electron-beam evaporation to deposit electrode metals. The gate electrode was a Ni/Au contact. The gate length and width were 1.5 and 20 $\mu$m, respectively. The source-drain spacing was 5 $\mu$m. The ohmic contact was Ti/Al/Ni/Au annealed at 850°C for 30 seconds. The DC characteristics were measured with a semiconductor parameter analyzer. Transmission line method (TLM) patterns were fabricated close to the devices for the estimation of the contact resistance.

## 3. Results and Discussion

First, we investigated the properties of the heterostructures. Figure 1 shows the sheet resistance ($R_{sh}$) and the rms (root
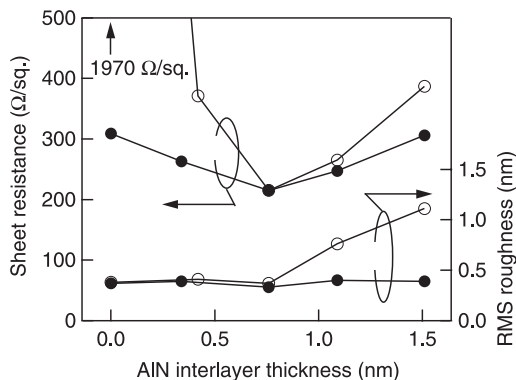


**Fig. 1** Sheet resistance and rms roughness of the surface as a function of AlN interlayer thickness. Open and closed circles show the data for InAlN/GaN and InAlN/AlGaN/GaN, respectively.

mean square) roughness of the InAlN/AlGaN/GaN heterostructures as a function of AlN interlayer thickness. The data for the conventional InAlN/GaN heterostructures are also indicated. The $R_{sh}$ and the rms roughness are sensitive to the AlN thickness in the conventional heterostructures. This is consistent with the results in Ref. [9]. In contrast, the variation of these parameters is smaller for the InAlN/AlGaN/GaN heterostructures.

For the conventional structures, the surface is flat and the rms roughness is about 0.35 nm when the AlN interlayer is less than 0.75 nm thick. The rms roughness, however, steeply increases from 0.35 to 1.2 nm as the interlayer thickness increases from 0.75 to 1.5 nm. This is attributed to roughening of the AlN interlayer. The lattice strain of AlN, which increases as it gets thicker due to the large lattice mismatch, enhances the surface roughening. For the InAlN/AlGaN/GaN, the surface stays smooth and low-rms roughness of 0.35 nm is obtained in the range of the AlN interlayer thickness from 0 to 1.5 nm. In this case, the rough surface in the AlN/GaN becomes smooth during AlGaN layer growth at a high temperature of 1000°C. Figure 2 shows the surface morphology of InAlN/GaN and InAlN/AlGaN/GaN with the AlN interlayer to the thickness of 0, 0.75, and 1.5 nm. Although the rms roughness for InAlN/GaN with 0.75-nm-thick AlN is equal to that for the sample without AlN, deep pits are generated in the InAlN surface on the 0.75-nm-thick AlN [Figs. 2(a) and (b)]. In contrast, such pits are not observed for InAlN/AlGaN/GaN with the 0.75-nm-thick AlN interlayer [Fig. 2(e)]. The thick AlN interlayer makes the InAlN surface rougher. A lot of large pits with the diameter of about 200 nm are observed in the surface of the conventional structure with the 1.5-nm-thick AlN interlayer [Fig. 2(c)]. The insertion of AlGaN can not prevent the generation of some pits when 1.5-nm-thick AlN are inserted [Fig. 2(f)].

The $R_{sh}$ widely ranges from 210 to 2000 $\Omega$/sq. for InAlN/GaN in the region of AlN thickness between 0 to 1.5 nm. In contrast, the variation of $R_{sh}$ is smaller for InAlN/AlGaN/GaN. The $R_{sh}$ only ranges from 215 to 310 $\Omega$/sq. as seen in Fig. 1. The lowest $R_{sh}$ of about

0 nm        0.75 nm        1.5 nm
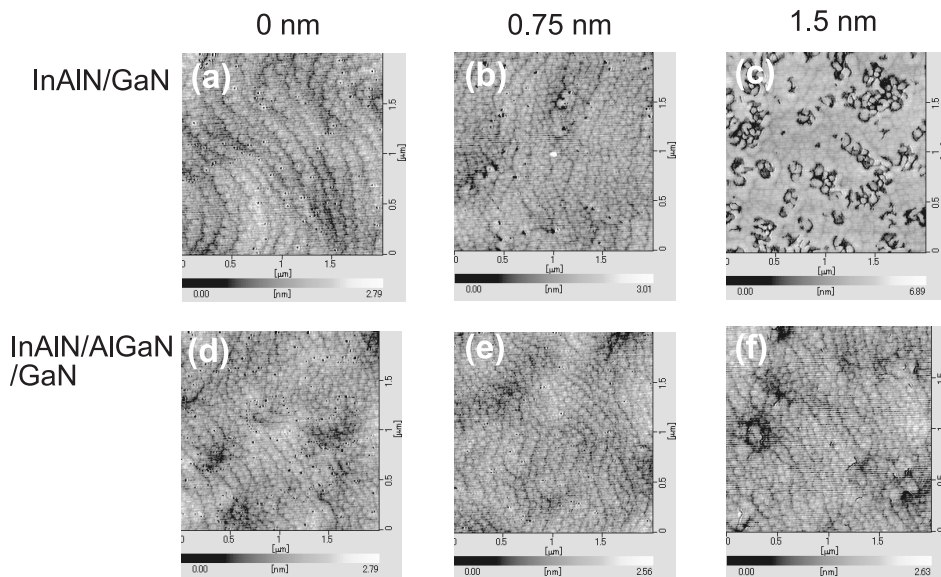


**Fig. 2** AFM images of surface morphologies of InAlN/GaN and InAlN/AlGaN/GaN heterostructures with 0-, 0.75-, and 1.5-nm-thick AlN interlayers.

210 $\Omega$/sq. is achieved for both structures with the AlN thickness of 0.75 nm. Figure 3 shows the electron mobilitiy and the $N_S$ as a function of the AlN interlayer thickness. For both structures, we obtained a large $N_S$ of 1.5–2.1 $\times$ $10^{13}$ cm$^{-2}$, resulting from the large spontaneous polarization charge of LM-InAlN. The $N_S$ of InAlN/AlGaN/GaN is smaller than that of InAlN/GaN. This indicates that the total polarization charge at the heterointerface is smaller for InAlN/AlGaN/GaN than for InAlN/GaN because the polarization charge of inserted $Al_{0.38}Ga_{0.62}N$ is smaller than that of LM-InAlN. The electron mobiltiy is higher for InAlN/AlGaN/GaN than for InAlN/GaN in the region of the AlN thickness. In addition, the variation is also smaller for InAlN/AlGaN/GaN. It was found that the variation of $R_{sh}$ corresponds to that of electron mobility. As mentioned above, the mobility of InAlN/GaN without the AlN interlayer is as low as 200 cm$^2$/V·s. In contrast, the insertion of AlGaN provides the high electron mobility of 1300 cm$^2$/V·s even without the AlN interlayer. This indicates that the alloy-disorder scattering rate in $Al_{0.38}Ga_{0.62}N$ is much smaller than that in InAlN. We achieved the highest electron mobility with the 0.75-nm-thick AlN interlayer for both structures. The values for InAlN/GaN and InAlN/AlGaN/GaN are 1470 and 1690 cm$^2$/V·s, respectively. As the AlN thickness increases from 0.75 to 1.5 nm, the mobility gradually decreases for both structures. The abruptness of heterointerface deteriorated as expected due to the rough surface as seen in Figs. 2(c) and (f). These results indicate that the insertion of AlGaN is effective for achieving a flat surface and abrupt heterointerface.

Next, we estimated the characteristics of the ohmic contact using TLM. Figures 4 and 5 show the TLM measurement results as a function of AlN interlayer thickness. The specific contact resistivity ($\rho_c$) is constant for the AlN
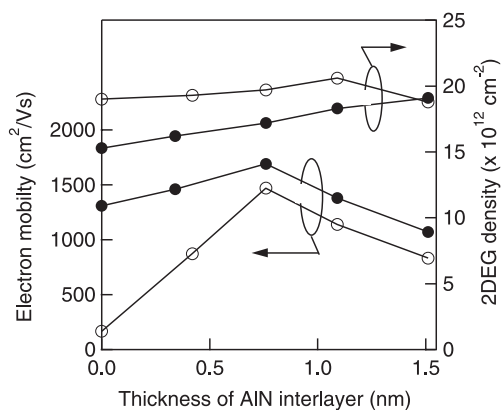


**Fig. 3** Electron mobility and 2DEG density of InAlN/GaN (open circles) and InAlN/AlGaN/GaN (closed circles) as a function of AlN interlayer thickness.
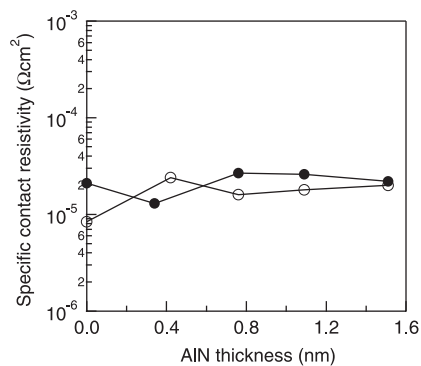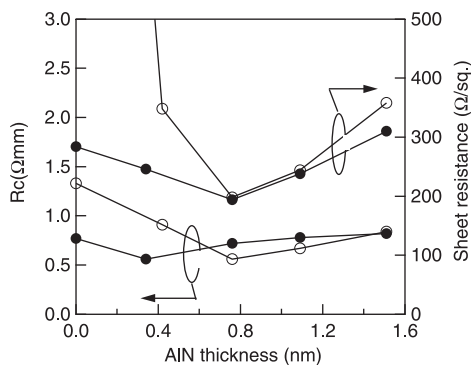


**Fig. 4** Specific contact resistivity of InAlN/GaN (open circles) and InAlN/AlGaN/GaN (closed circles) as a function of AlN interlayer thickness.
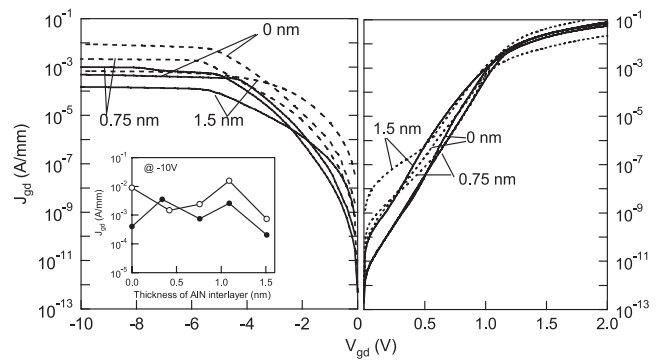
interlayer thickness as seen in Fig. 4. The value of around $1 \times 10^{-5}$ $\Omega cm^2$ is large compared with that for AlGaN/GaN heterostructures. This is attributed to the large barrier height of LM-InAlN or surface states. In spite of the large $\rho_c$, we obtained a low contact resistance ($R_c$) of less than 1 $\Omega$mm for all of the samples except InAlN/GaN with a 0- or 0.35-nm-thick AlN interlayer (Fig. 5). The low $R_{sh}$ of below 300 $\Omega$/sq. contributes to the low $R_c$, i.e., $R_c = \sqrt{\rho_c \cdot R_{sh}}$. If we make $\rho_c$ lower, signicantly low $R_c$ can be achieved. Si doping technology and surface treatment should be investigated in future work in order to reduce $\rho_c$.

Then, we measured the gate leakage characteristics. Figure 6 shows forward and reverse gate lekage current of InAlN/GaN and InAlN/AlGaN/GaN with a 0-, 0.75-, or 1.5-nm-thick AlN interlayer. The leakage current of InAlN/AlGaN/GaN tends to be smaller than that of In-

AlN/GaN for each AlN thickness. This is consistent with the previous results for heterostructures with a 1-nm-thick AlN interlayer [13]. This smaller leakage seem to be due to the smoother surface for the InAlN/AlGaN/GaN. If this is corrected, the leakage current should increase with increasing AlN thickness for InAlN/GaN whose surface become rougher. However, a clear correlation was not found as seen in the inset of Fig. 6. The reason for the smaller leakage for InAlN/AlGaN/GaN is not clear at present; however, the inserted AlGaN layers probably reduce it. The barrier height of LM-InAlN should be larger than that of the conventional AlGaN with the Al content of 0.2–0.3. However, the leakage current is comparable with that of AlGaN. This is probably due to tunneling current caused by surface traps or by large



**Fig. 6** Gate leakage current of the samples with 0-, 0.75-, and 1.5-nm-thick AlN interlayers. Dotted lines and solid lines show the current of InAlN/GaN and InAlN/AlGaN/GaN, respectively. Inset shows the reverse leakage current at $V_{gd} = -10$ V as a function of the AlN interlayer thickness. Open circles and closed circles show the data for InAlN/GaN and InAlN/AlGaN/GaN, respectively.
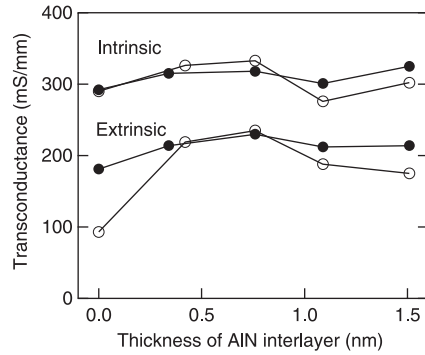


**Fig. 5** Contact resistance and sheet resistance of InAlN/GaN (open circles) and InAlN/AlGaN/GaN (closed circles) as a function of AlN interlayer thickness.
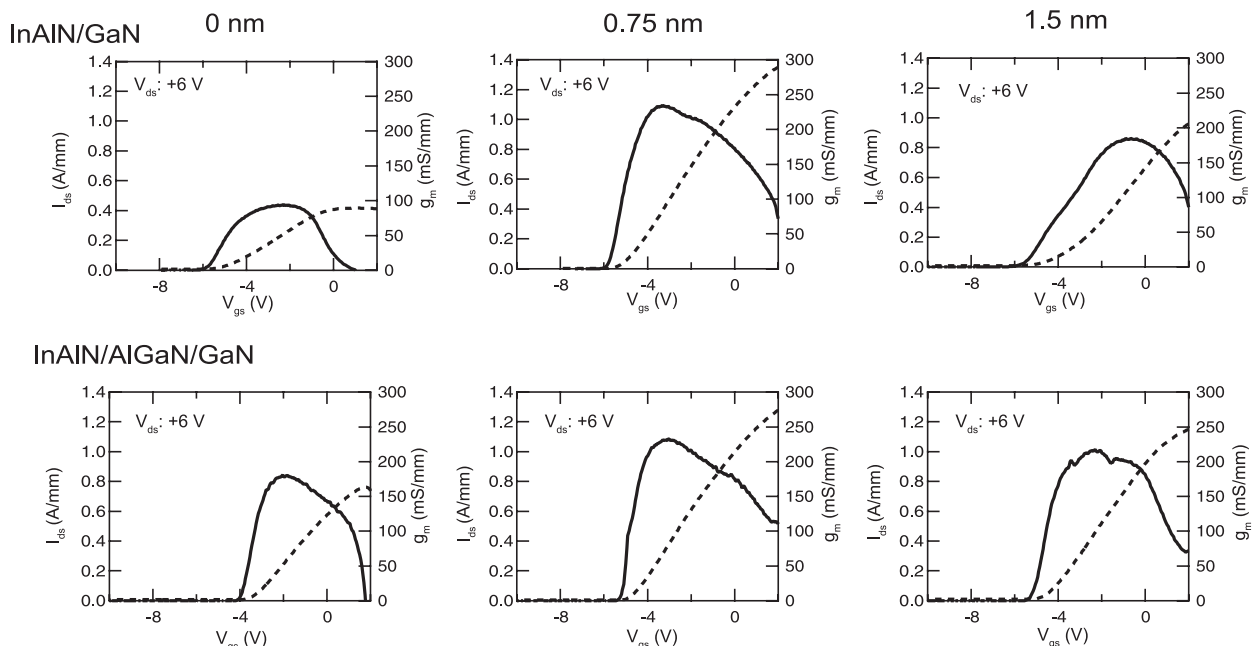


**Fig. 7** Transfer characteristics of InAlN/GaN and InAlN/AlGaN/GaN heterostructures FETs with 0-, 0.75-, and 1.5-nm-thick AlN interlayers.

**Fig. 8** Intrinsic and extrinsic maximum transconductance as a function of AlN interlayer thickness. Open circles and closed circles show the data for InAlN/GaN and InAlN/AlGaN/GaN, respectively.

polarization charge. We need to optimize the growth condition of InAlN, and the surface treatment prior gate electrode deposition should also be improved.

Finally, we examined the DC characteristics of FETs. Figure 7 shows the transfer characteristics of InAlN/GaN and InAlN/AlGaN/GaN HFETs with a 0-, 0.75-, or 1.5-nm-thick AlN interlayer. The threshold voltage of InAlN/GaN of about $-5$ V for InAlN/AlGaN/GaN is shallower than those of $-6$ V for InAlN/GaN, resulting from the smaller $N_S$ for InAlN/AlGaN/GaN. Large drain current of 1.2 A/mm was obtained for both structures with the 0.75-nm-thick AlN interlayer because of the low access resistance of 200 $\Omega$/sq. The slope of the drain current at the threshold voltage is larger for InAlN/AlGaN/GaN than for InAlN/GaN with each AlN thickness. This is attributed to the high electron mobility for InAlN/AlGaN/GaN at low electric field.

The AlN interlayer thickness also affects the device characteristics. Figure 8 shows the dependence of maximum transconductance ($g_m$) on AlN interlayer thickness for the two heterostructures FETs. The maximum $g_m$ of the InAlN/AlGaN/GaN FETs is nearly constant and about 200 mS/mm, resulting from the small variation of $R_{sh}$ and $R_c$. The $g_m$ of InAlN/GaN FETs with the AlN interlayer is also around 200 mS/mm. In contrast, $g_m$ is as low as 100 mS/mm for InAlN/GaN when the AlN interlayer is not inserted. The intrinsic maximum $g_m$ values estimated from end-resistance measurements are also shown in Fig. 8. The value of 300 mS/mm for the InAlN/GaN without the interlayer is equal to the values for other samples with the interlayer, which indicates that only high $R_c$ is responsible for the low $g_m$. The low electron mobility does not contribute to the transconductance at high electric field.

## 4. Conclusion

We investigated the influence of the thickness of the AlN interlayer for InAlN/GaN and InAlN/AlGaN/GaN heterostructures. The AlN thickness strongly affects the mobility and the surface roughness of InAlN/GaN. In contrast, its effect is suppressed for InAlN/AlGaN/GaN heterostruc-

tures. We achieved low sheet resistance of 310 $\Omega$/sq. even without an AlN interlayer. We found that the influence of AlN thickness for InAlN/AlGaN/GaN FETs is smaller than that for InAlN/GaN FETs. Although the $\rho_c$ and gate leakage should be improved, these results indicate that the InAlN/AlGaN/GaN heterostructures could lead to development of the performance of GaN-based FETs.

## Acknowledgments

### References

[1] A. Bykhovski, B. Gelmont, and M. Shur, "The influence of the strain-induced electric field on the charge distribution in GaN-AlN-GaN structure," J. Appl. Phys., vol.74, no.11, pp.6734–6739, 1993.

[2] F. Bernardini and V. Fiorentini, "Spontaneous polarization and piezoelectric constants of III-V nitrides," Phys. Rev. B, vol.56, no.16, pp.10024–10027, 1997.

[3] J. Kuzmík, "Power electronics on InAlN/(In)GaN: Prospect for a record performance," IEEE Electron Device Lett., vol.22, no.11, pp.510–512, 2001.

[4] O. Ambacher, R. Dimitrov, M. Stutzmann, B.E. Foutz, M.J. Murphy, J.A. Smart, J.R. Shealy, N.G. Weimann, K. Chu, M. Chumbes, B. Green, A.J. Sierakowski, W.J. Schaff, and L.F. Eastman, "Role of spontaneous and piezoelectric polarization induced effects in group-III nitride based heterostructures and devices," Phys. Status Solidi b, vol.216, no.1, pp.381–389, 1999.

[5] A. Koukitu, Y. Kumagai, and H. Seki, "Thermodynamic analysis of the MOVPE growth of InAlN," Phys. Status Solidi a, vol.180, no.1, pp.115–120, 2000.

[6] V.W.L. Chin, B. Zhou, T.L. Tansley, and X. Lin, "Alloy-scattering dependence of electron mobility in the ternary gallium, indium, and aluminum nitrides," J. Appl. Phys., vol.77, no.11, pp.6064–6066, 1995.

[7] M. Higashiwaki and T. Matsui, "InAlN/GaN heterostructure field-effect transistors grown by plasma-assisted molecular-beam epitaxy," Jpn J. Appl. Phys, vol.43, pp.L768–L770, 2004.

[8] A. Dadgar, F. Schulze, J. Bläsing, A. Diez, A. Krost, M. Neuburger, E. Kohn, I. Daumiller, and M. Kunze, "High-sheet-charge–carrier-density AlInN/GaN field-effect transistors on Si(111)," Appl. Phys. Lett., vol.85, no.22, pp.5400–5402, 2004.

[9] M. Gonschorek, J.F. Carlin, E. Feltin, M.A. Py, and N. Grandjean, "High electron mobility lattice-matched AlInN/GaN field-effect transistor heterostructures," Appl. Phys. Lett., vol.89, no.6, 062106, 2006.

[10] I.P. Smorchkova, L. Chen, T. Mates, L. Shen, S. Heikman, B. Moran, S. Keller, S.P. DenBaars, J.S. Speck, and U.K. Mishra, "AlN/GaN and (Al,Ga)N/AlN/GaN two-dimensional electron gas structures grown by plasma-assisted molecular-beam epitaxy," J. Appl. Phys., vol.90, no.10, pp.5196–5201, 2001.

[11] L. Shen, S. Heikman, B. Moran, R. Coffie, N.Q. Zhang, D. Buttari, I.P. Smorchkova, S. Keller, S.P. DenBaars, and U.K. Mishra, Al-GaN/AlN/GaN high-power microwave HEMT. IEEE Electron Device Lett., vol.22, no.10, pp.457–459, 2001.

[12] M. Hiroki, N. Maeda, and T. Kobayashi, "Fabrication of an In-AlN/AlGaN/AlN/GaN heterostructure with a flat surface and high electron mobility," Appl. Phys. Express., vol.1, no.11, 111102, 2008.

[13] M. Hiroki, N. Maeda, and T. Kobayashi, "Electrical properties

and device characteristics of InAlN/AlGaN/ AlN/GaN heterostructure field effect transistors," Phys. Status Solidi c, vol.6, no.S2, pp.S1056–S1060, 2009.

[14] R. Coffie, Y.C. Chen, I. Smorchkova, M. Wojtowicz, Y.C. Chou, B. Heying, and A. Oki, "Impact of AlN interlayer on reliability of AlGaN/GaN HEMTs," 2006 IEEE International Reliability Physics Symposium proceedings. 44th Annual, pp.99–102, 2006.

**Masanobu Hiroki** received the B.S. and M.S. degrees in physics from Osaka University in 1998, 2000, respectively. In 2000, he joined NTT Basic Research Laboratories, NTT Corporation, Kanagawa, Japan. Since then, he has been engaged in the research and development on the crystal growth of nitride semiconductors. Currently, he is working on the crystal growth for nitride-based electron devices at NTT Photonics Laboratories, NTT Corporation, Kanagawa, Japan. Mr. Hiroki is a member of The Japan Society of Applied Physics.

**Narihiko Maeda** received the B.S., M.S., and Ph.D. degrees in applied physics from The University of Tokyo in 1985, 1987, and 1990, respectively. In 1990, he joined NTT Basic Research Laboratories, NTT Corporation, Tokyo, Japan. Since then, he has been engaged in the research and development on the crystal growth and electron devices of III-V compound semiconductors. Currently, he is working on nitride-based electron devices at NTT Photonics Laboratories, NTT Corporation, Kanagawa, Japan. Since 2007, he has served a guest researcher of Institute of Industrial Science, The University of Tokyo, Japan. Since 2007, he has been a guest professor at Ritsumeikan Universiy, Shiga, Japan. Dr. Maeda is a member of The Japan Society of Applied Physics, The Physical Society of Japan, and Materials Research Society.

**Naoteru Shigekawa** received the B.S., M.S., and Ph.D. degrees in physics from the University of Tokyo, Japan, in 1984, 1986, and 1993, respectively. He joined Atsugi Electrical Communications Laboratories, Nippon Telegraph and Telephone Corporation (NTT), Kanagawa, Japan, in 1986, and was engaged in research of hot carrier transport in III-V compound-semiconductor heterostructures. From 1993 to 1994, he was a Visiting Scientist at the Department of Physics, University of Nottingham, U.K., where he worked on resonant-tunnelling heterojunction bipolar transistors. Currently, he is with NTT Photonics Laboratories, Kanagawa. His current research interests are transport properties in compound semiconductor heterostructures and electron devices. Dr. Shigekawa is a member of the Physical Society of Japan, the Japan Society of Applied Physics, the American Physical Society, the Institute of Physics, and IEEE.